THE ASTROPHYSICAL JOURNAL, 431:123–136, 1994 August 10


# MISDIRECTED QUASARS AND EVOLVED STARS IN DISTANT RADIO GALAXIES[1]

SPERELLO DI SEREGO ALIGHIERI
Osservatorio Astrofisico di Arcetri, Largo E. Fermi 5, I-50125, Firenze, Italy; sperello@arcetri.astro.it

ANDREA CIMATTI
European Southern Observatory, Karl-Schwarzschild-Strasse 2, D-8046, Garching bei München, Germany; acimatti@eso.org; and
Dipartimento di Astronomia, Universitá di Firenze, Italy

AND

ROBERT A. E. FOSBURY[2]
Space Telescope–European Coordinating Facility, Karl-Schwarzschild-Strasse 2, D-85748, Garching bei München, Germany;
rfosbury@eso.org

*Received 1993 December 3; accepted 1994 February 4*

## ABSTRACT

We present the results of spectropolarimetry of radio galaxies with redshift close to 1, complemented by imaging polarimetry. These show: (1) a flat (in $f_\lambda$) polarized UV continuum, (2) broad polarized Mg II emission line, (3) narrow unpolarized forbidden emission lines, (4) a drop in the polarization of the continuum to the red of 4000 Å, (5) a strong absorption feature at 2598 Å, and (6) perpendicularity between the $\boldsymbol{E}$ vector of polarization, as measured with imaging polarimetry, and the optical/radio axis. These data provide evidence that distant radio galaxies harbor a quasar which is hidden from direct view but seen by scattering from the interstellar medium in the galaxy. Hot electrons cannot be the dominant scattering agent because of the presence of polarized Mg II lines with a width similar to that observed in quasars. The drop in the continuum polarization to the red of the 4000 Å break suggests dilution by a red stellar population. The absorption line at 2598 Å is probably due to interstellar Fe II. We discuss a two-component model consisting of a dust scattered quasar and an evolved stellar population, which reproduces simultaneously the polarization measurements and the UV/optical spectral energy distribution. Our results provide strong observational support to the unified model for the most luminous active galactic nuclei and to the idea that the alignment effect in distant radio galaxies is due to scattering, and they add an important tool for the study of the early evolution of galaxies.

*Subject headings:* galaxies: evolution — line: identification — polarization — quasars: general — ultraviolet: galaxies

## 1. INTRODUCTION

In the simplest form of the unified model of active galactic nuclei (AGNs) (see Antonucci 1993 for a recent review), a type 1 spectrum—consisting of a featureless continuum and broad emission lines—is emitted anisotropically from the nuclear regions in two oppositely directed cones which are the result of shadowing by obscuration close to source of radiation. This type 1 spectrum is visible directly only if our line of sight falls within the opening angle of the cones. For objects with axes closer to the plane of the sky, an indirect view of the central regions is provided by scattering, as has been beautifully demonstrated by the presence of a polarized type 1 spectrum in a few nearby AGNs (e.g., NGC 1068; see Miller, Goodrich, & Mathews 1991). For the radio-loud AGNs (quasars and powerful radio galaxies), there is evidence for relativistic beaming which provides an additional "intrinsic" anisotropy with what is likely to be a much narrower opening angle. Statistical studies of the radio angular sizes in a complete sample of extragalactic radio sources (Barthel 1989) and of the luminosity functions of complete samples of radio-loud AGNs (Padovani & Urry 1992 and references therein) suggest that the powerful radio galaxies form the parent population of the radio quasars and blazars. The presence of a scattered type 1 spectrum in distant radio galaxies is, however, still a matter of debate (e.g., Chambers & Miley 1990; Meisenheimer & Hippelein 1992), but its unequivocal detection would greatly support the unified models for the most luminous AGNs, providing clues to the mechanisms for anisotropic emission and enabling a clean separation of the stellar light in the host galaxies, leading to a determination of stellar ages at cosmologically important distances. The details of the scattering process in the restframe ultraviolet (UV), where dust scattering is strong and starlight is weak, can also provide interesting constraints on the properties of dust in extreme environments and at early epochs.

The discovery of perpendicular polarization in distant radio galaxies (di Serego Alighieri et al. 1989; see also Cimatti et al. 1993 for a recent review) is a strong indication of the presence of scattered nuclear radiation, but, since it results from broad-band imaging polarimetry, it gives little information on the scattered spectrum. In particular, the results cannot be used to distinguish between a quasar- or a blazar-like spectrum for the anisotropic nuclear radiation. Although the scattering hypothesis has provided a consistent explanation of the alignment effect—i.e., the fact that the rest frame UV radiation of high-redshift radio galaxies is elongated and aligned with their radio axes—a detailed understanding of the wavelength dependence of the polarization is still required to constrain the presence of blue light from young stars (see Cimatti et al. 1993; McCarthy 1993 for recent reviews of the problem).

We have therefore started a program of spectropolarimetry

[1] Based on observations obtained at the European Southern Observatory, La Silla, Chile.

[2] Affiliated to the Astrophysics Division of the Space Science Department, European Space Agency.

TABLE 1

RESULTS OF IMAGING POLARIMETRY

| Galaxy | $z$ | Date | Band | Magnitude | $\Delta\lambda_{rest}$ (Å) | Polarization$_{obs}$ | $\theta$ | $\Delta\theta_{opt}$ | Polarization$_{cont.}$[a] | Reference |
|---|---|---|---|---|---|---|---|---|---|---|
| 3C 226..... | 0.818 | 1991 Jun | *B* | ... | 2150–2700 | 12.3% ± 2.3% | 49° ± 6° | 86° ± 7° | ... | (1) |
| | | 1991 Jan | *V* | 21.7 | 2650–3400 | 13.3 ± 4.2 | 41 ± 9 | 86 ± 9 | ... | (2) |
| | | 1993 Mar | *i* | 20.4 | 4000–4800 | 2.5 ± 1.4 | 51 ± 13 | 84 ± 13 | 2.9% | (3) |
| 3C 227.2..... | 0.766 | 1989 Apr | *B* | 22.0 | 2200–2800 | 21.0 ± 4.0 | 164 ± 6 | 86 ± 6 | ... | (4) |
| | | 1993 Mar | *i* | 20.5 | 4100–4900 | 7.3 ± 1.4 | 169 ± 7 | 89 ± 8 | 9.9 | (3) |
| 3C 324..... | 1.206 | 1991 Jun | *R* | 21.7 | 2450–3400 | 18.0 ± 1.6 | 16 ± 5 | 78 ± 6 | ... | (1) |

[a] Continuum polarization corrected for dilution by forbidden line emission (see § 3.1).

REFERENCES.—(1) di Serego Alighieri et al. 1993; (2) Tadhunter et al. 1992; (3) this work; and (4) di Serego Alighieri et al. 1989.

of distant radio galaxies with the aim of studying the nature of the scattered radiation, understanding the scattering mechanism, and disentangling the spectral energy distribution of the stellar radiation. We present here the first results for three radio galaxies with redshift around one.

## 2. OBSERVATIONS AND ANALYSIS

The three targets were selected from among the most distant radio galaxies having existing polarization measurements (Cimatti et al. 1993). This was in order to exploit the knowledge of the orientation of the ***E*** vector as a way of maximizing the information return from the very time-consuming spectropolarimetric observations. Table 1 summarizes the previously known optical polarization measurements on the observed galaxies and also includes the results of the imaging polarimetry described in § 3.1. The new observations described in this paper were all carried out in 1993 March, using the ESO 3.6 m telescope in La Silla (Chile) equipped with the ESO Faint Object Spectrograph and Camera (EFOSC1; see Melnick, Dekker, & D'Odorico 1989) in its imaging polarimetry and spectropolarimetry modes. The new imaging polarimetry has been carried out primarily to extend the wavelength range covered by the spectropolarimetry.

### 2.1. *Imaging Polarimetry*

The two galaxies 3C 226 and 3C 277.2 were observed with EFOSC1, in imaging polarimetry mode with the Gunn *i* filter, in order to extend measurements above the 4000 Å break. No such observations were made for 3C 324 since, for this object, the 4000 Å break falls to the red of the *i* filter, where the CCD sensitivity is falling rapidly. The technique used for observations and data reduction is described in detail by di Serego Alighieri 1989 (see also di Serego Alighieri, Cimatti, & Fosbury 1993) and is not repeated here. We only recall that our method is free from the effects of any time variation of the observing conditions, such as seeing and instrumental polarization, because the polarization is derived from the ratio of intensities measured on the *same* frame. Furthermore, instrumental polarization (always lower than 1%) is corrected for using field stars measured on the same frame as the target galaxy. Three exposures of 30 minutes each at the EFOSC1 position angles 285°, 315°, and 345° and four exposures of 30 minutes at position angles 255°, 285°, 315°, and 345° were made for 3C 226 and 3C 277.2, respectively. Seeing conditions were moderate with the FWHM ranging between 1.″1 and 1.″5. The photometric calibration was derived from observations of the spectrophotometric standard star Kopff 27.

### 2.2. *Spectropolarimetry*

Spectropolarimetry is achieved with EFOSC1 by inserting both a grism and the Wollaston prism in the parallel beam. For each object in the slit, this produces two orthogonally polarized spectra separated by 10″ in the direction of the slit, perpendicular to the dispersion. In order to prevent overlap of the spectra and to reduce the sky contribution, the slit—which was 2″ wide—was masked with 11″ wide opaque bars alternating with 9″ openings. This results in 10 9″ × 2″ free sections of the slit, one of which is used for the target galaxy and the rest for the sky and for field stars. Each section produces two nonoverlapping and perpendicularly polarized spectra on the CCD. The intensity ratio of the two spectra provides a measurement of the component $S(\phi)$ of the normalized Stokes parameters describing the linear polarization, along the direction of the Wollaston prism position angle[3] $\phi$, much in the same way as for imaging polarimetry (di Serego Alighieri 1989). The value of the degree of linear polarization $P(\lambda)$ and of the position angle $\theta(\lambda)$ of the plane of vibration of the ***E*** vector can be derived from a minimum of two spectra taken at different position angles $\phi$, since

$$S(\phi, \lambda) = P(\lambda) \cos 2[\theta(\lambda) - \phi] . \quad (1)$$

Since EFOSC1 was not yet equipped with a half-wave plate, one had to change $\phi$ by a rotation of the whole instrument, including the slit. This means that different parts of an extended object would be selected at each angle. In order to circumvent this problem, we have *assumed* that the direction of the ***E*** vector is constant with wavelength and equal to the value measured with imaging polarimetry, i.e., perpendicular to the elongation in the optical structure. For 3C 226 and 3C 277.2 this assumption is justified by the actual measurements of $\theta(\lambda)$ made with imaging polarimetry in three and two different bands, respectively, and covering the wavelength range of the spectra (Table 1). We have therefore used all of the available spectropolarimetric telescope time to obtain spectra at a single position angle $\phi$ equal to the assumed $\theta$. This means that the slit was aligned with the optical elongation and therefore accepted a large fraction of the light from the galaxy, including the aligned extended structure. If our assumption is correct, then equation (1) says that $P(\lambda) = S(\theta, \lambda)$, which means that we can derive the value of $P(\lambda)$ from our observations taken at a single position angle $\phi = \theta$. Therefore, in the following we will quote measurements of $P(\lambda)$, while formally we have measured

[3] We define the position angle $\phi$ of the Wollaston prism as perpendicular to the plane which contains the two output beams from the prism. Therefore, in our configuration the slit is perpendicular to $\phi$.

TABLE 2

SPECTROPOLARIMETRIC OBSERVATIONS

| Galaxy | Grism | $\Delta\lambda_{rest}$ (Å) | Exposure Time (minutes) | Slit P.A. |
|---|---|---|---|---|
| 3C 226..... | B300 | 2250–3700 | 45 | 44° |
| | B300 | 2250–3700 | 45 | 135 |
| 3C 277.2..... | B300 | 2250–3700 | 2 × 40 | 73 |
| 3C 324..... | R300 | 2650–4350 | 2 × 40 | 90 |

$S(\theta, \lambda)$. In any case, this will be a lower limit to $P(\lambda)$. We stress that our observing strategy, admittedly not leading to a complete determination of $P(\lambda)$, was necessary to obtain spectropolarimetric information on our faint targets with a 4 m class telescope without exceeding the observing time normally allocated on these facilities.

The parameters of the spectropolarimetric observations are given in Table 2. We have used the blue grism B300 for 3C 226 and 3C 277.2 and the red grism R300 for 3C 324 to include Mg II $\lambda$2798 and [O II] $\lambda$3727 in the spectra. The spectrophotometric standard stars Kopff 27 (Stone 1977) and EG 274 (Stone & Baldwin 1983; Baldwin & Stone 1984) were observed with the same setup, i.e., with the grism, Wollaston prism, and slotted slit. These provided both the absolute flux calibration and the first-order correction for the instrumental polarization. The latter includes all the effects originating in EFOSC1, e.g., those due to the grism and to the CCD, and is measured to be about 5%. All other effects contributing to the instrumental polarization, e.g., those due to the telescope and to the atmosphere, have been evaluated in the following way.

In the case of 3C 226, which is barely resolved, the slit was oriented along the small optical elongation in the first exposure and perpendicular to it in the second one. For the polarization measurement this results in an interchange of the two perpendicularly polarized spectra produced by the Wollaston prism and therefore provides data for the elimination of any residual instrumental polarization. The fact that the intensity ratio of the two spectra was indeed inverted in the two exposures indicates that the residual instrumental polarization is negligible. For the second exposure of 3C 226 and for both exposures of 3C 324 the slit position was slightly adjusted to include a faint field star in one of the free slit sections. For this star, which is assumed to be unpolarized, $S(\phi) < 0.01$ at all wavelengths.

A further check on the observing and analysis procedure is provided by the observations of the polarimetric standard star HD 16121 performed with the Wollaston prism and both grisms with the slit perpendicular to the known direction of the $E$ vector (P.A. = 2°). The measured polarization [formally $S(\phi, \lambda)$] is shown in Figure 1 and corresponds very well to a Serkowski interstellar polarization curve (Serkowski, Mathewson, & Ford 1975) with $P_{max} = 7.9\%$ and $\lambda_{max} = 5450$ Å. These values are close to those given by Serkowski et al. (1975) ($P_{max} = 6.77 \pm 0.12\%$, and $\lambda_{max} = 5300 \pm 100$ Å), who obtained them from the broadband $U$, $B$, $V$ polarization measurements of Visvanathan (1966). The good agreement of our data with the Serkowski curve and the excellent correspondence of our results obtained with different grisms in the overlap region (5800–6700 Å) confirm the reliability our spec-

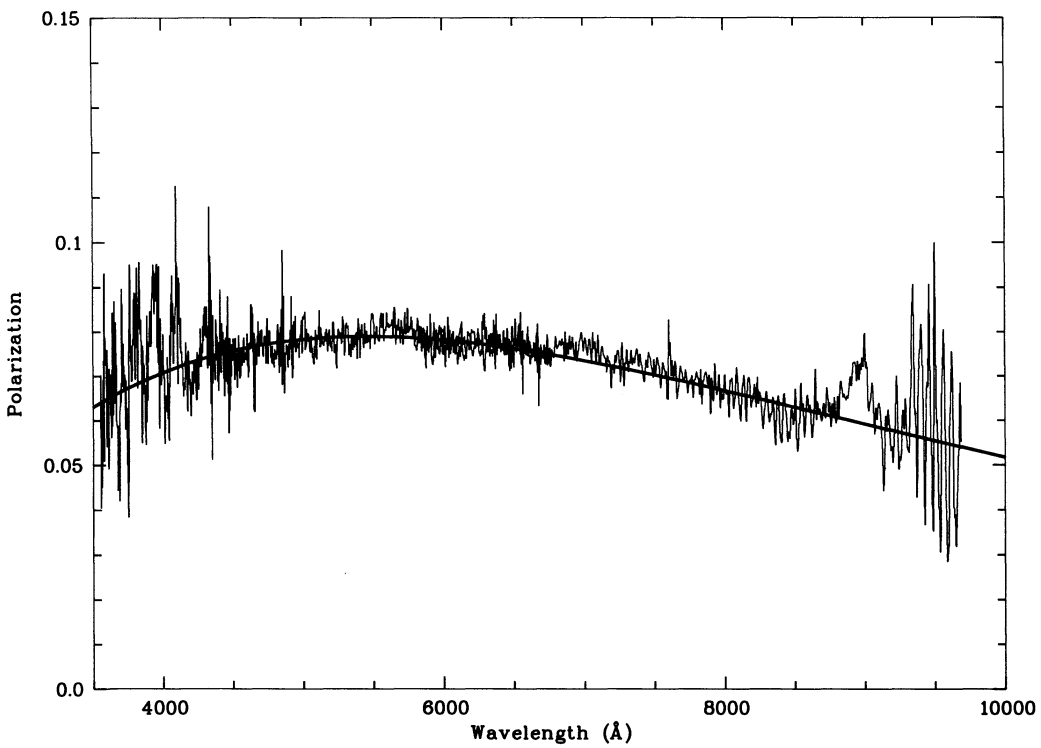


FIG. 1.—The degree of linear polarization [formally $S(\phi, \lambda)$] for the spectropolarimetric standard star HD 161291. The thick line is a Serkowski et al. (1975) interstellar polarization curve for $P_{max} = 7.9\%$ and $\lambda_{max} = 5450$ Å.

tropolarimetry results, at least in the range 4300–8800 Å, where the sensitivity of EFOSC1 is high.

## 3. RESULTS

### 3.1. *Broadband Polarimetry*

The results of the Gunn *i*-band polarimetry of 3C 226 and 3C 277.2 are summarized in Table 1 and refer to the whole galaxy integrated over an aperture of about 20 arcsec$^2$ for both objects. The listed degree of polarization has been corrected for the bias at low levels (Wardle & Kronberg 1974; Clarke & Stewart 1986). The quoted errors on the degree of polarization $P$ and position angle $\theta$ have been determined using a stochastic model of the observing process (Fosbury, Cimatti, & di Serego Alighieri 1993, 1994). This accounts correctly for the fact that the distribution functions of these quantities, particularly $P$, are nonnormal.

We remark on the constancy of the direction of polarization with wavelength, which is a strong indication that just a single polarization mechanism is at work. Also note the sudden decrease of the degree of polarization redward of the 4000 Å break. The Gunn *i* band contains some permitted emission lines (H$\beta$, H$\gamma$, H$\delta$, and He II $\lambda$4686) and two strong forbidden lines ([O III] 4959 + 5007). To obtain the continuum polarization in this band, the observed polarization must be corrected for the effects of emission lines, but only as far as the narrow component is concerned, since the broad one, if it exists, is probably polarized (see § 3.3). According to the typical line ratios observed in radio galaxies (McCarthy 1993) and to the transmission curve of the Gunn *i* filter, we estimate that the narrow lines contribute 14% and 27% of the total *i* flux for 3C 226 and 3C 277.2, respectively. If the narrow lines are unpolarized, as it is likely (see § 3.4), the values of $P$ are increased slightly, as shown in Table 1.

### 3.2. *The Polarization of the Continuum*

The signal-to-noise ratio of the spectra taken with the Wollaston prism precludes the measurement of polarization for every pixel, corresponding to about 3.5 Å in the rest frame. Therefore, the spectra have been resampled into wider wavelength bins selected to avoid the object emission lines and strong sky features. The results are given in Table 3 and Figure 2 and have not been corrected for the usual polarization bias. This is because they are actually a measurement of the Stokes parameter $S(\theta)$, which, to a sufficient approximation, has a symmetric distribution function. The quoted uncertainties in this case were evaluated analytically from the Poisson noise in the object and the sky background. Table 3 also contains the polarization measured in our spectra over bins corresponding to the broad bands of the previous imaging polarimetry listed in Table 1. The comparison is satisfactory.

### 3.3. *Broad Permitted Lines*

If misdirected quasars are present in distant radio galaxies, we should see polarized broad lines in their spectra, as has been observed for the low-redshift radio galaxy 3C 234 at $z = 0.185$ (Antonucci 1984). The spectra obtained so far have either not been of sufficient signal-to-noise ratio or have not covered the appropriate wavelength range to definitively answer this ques-

TABLE 3

SPECTROPOLARIMETRY OF THE CONTINUUM

| Galaxy | $\Delta\lambda_{rest}$ (Å) | $F_\lambda$ ($10^{-18}$ ergs s$^{-1}$ cm$^{-2}$ Å$^{-1}$) | Polarization$_{obs}$ | $F_{\lambda,Pol}$ ($10^{-19}$ ergs s$^{-1}$ cm$^{-2}$ Å$^{-1}$) |
|---|---|---|---|---|
| 3C 226..... | 2105–2305 | 3.45 ± 0.23 | 13.5% ± 4.9% | 4.6 ± 1.7 |
| | 2455–2585 | 4.62 ± 0.20 | 12.3 ± 3.1 | 5.7 ± 1.4 |
| | 2625–2725 | 4.94 ± 0.18 | 13.3 ± 2.7 | 6.6 ± 1.3 |
| | 2745–2845[a] | 5.90 ± 0.18 | 11.7 ± 2.2 | 6.9 ± 1.3 |
| | 2890–3045 | 4.67 ± 0.15 | 8.9 ± 2.3 | 4.2 ± 1.1 |
| | 3105–3195 | 5.05 ± 0.21 | 9.7 ± 3.0 | 4.9 ± 1.5 |
| | 3265–3335 | 5.45 ± 0.28 | 10.9 ± 3.2 | 5.9 ± 1.7 |
| | 3515–3585 | 5.56 ± 0.25 | 7.6 ± 3.3 | 4.2 ± 1.8 |
| | 3630–3695 | 5.09 ± 0.23 | 11.0 ± 3.1 | 5.6 ± 1.6 |
| | 2150–2740[b] | 4.19 ± 0.10 | 14.6 ± 1.7 | 6.1 ± 0.7 |
| | 2650–3400[c] | 5.28 ± 0.07 | 12.1 ± 1.0 | 6.4 ± 0.5 |
| 3C 277.2..... | 2035–2270 | 2.21 ± 0.19 | ... | ... |
| | 2440–2520 | 3.93 ± 0.30 | 16.4 ± 3.5 | 6.4 ± 1.4 |
| | 2610–2715 | 4.85 ± 0.26 | 23.5 ± 2.4 | 11.4 ± 1.2 |
| | 2750–2850[a] | 6.36 ± 0.24 | 19.5 ± 1.8 | 12.5 ± 1.2 |
| | 2965–3100 | 5.25 ± 0.22 | 13.9 ± 2.3 | 7.3 ± 1.2 |
| | 3240–3330 | 5.52 ± 0.24 | 16.0 ± 2.3 | 8.8 ± 1.3 |
| | 3465–3540 | 5.24 ± 0.27 | 22.9 ± 2.2 | 12.0 ± 1.2 |
| | 3625–3700 | 5.48 ± 0.25 | 13.0 ± 2.4 | 7.2 ± 1.3 |
| | 3765–3820 | 5.00 ± 0.28 | 18.4 ± 2.6 | 9.2 ± 1.3 |
| | 2210–2805[b] | 4.42 ± 0.20 | 24.2 ± 3.0 | 10.7 ± 1.3 |
| 3C 324..... | 2710–2780 | 3.03 ± 0.29 | 14 ± 6 | 4.2 ± 1.8 |
| | 2780–2825[a] | 5.48 ± 0.31 | 7 ± 4 | 3.8 ± 2.2 |
| | 3000–3090 | 2.90 ± 0.22 | 9 ± 5 | 2.6 ± 1.5 |
| | 3170–3275 | 3.90 ± 0.22 | 14 ± 4 | 5.4 ± 1.6 |
| | 3650–3700 | 3.14 ± 0.37 | 11 ± 7 | 3.5 ± 2.2 |
| | 2625–3400[d] | 3.47 ± 0.10 | 14 ± 3 | 4.9 ± 1.1 |

[a] Both continuum and Mg II 2798 are included.
[b] Corresponds to the *B*-band imaging polarimetry.
[c] Corresponds to the *V*-band imaging polarimetry.
[d] Corresponds to the *R*-band imaging polarimetry.

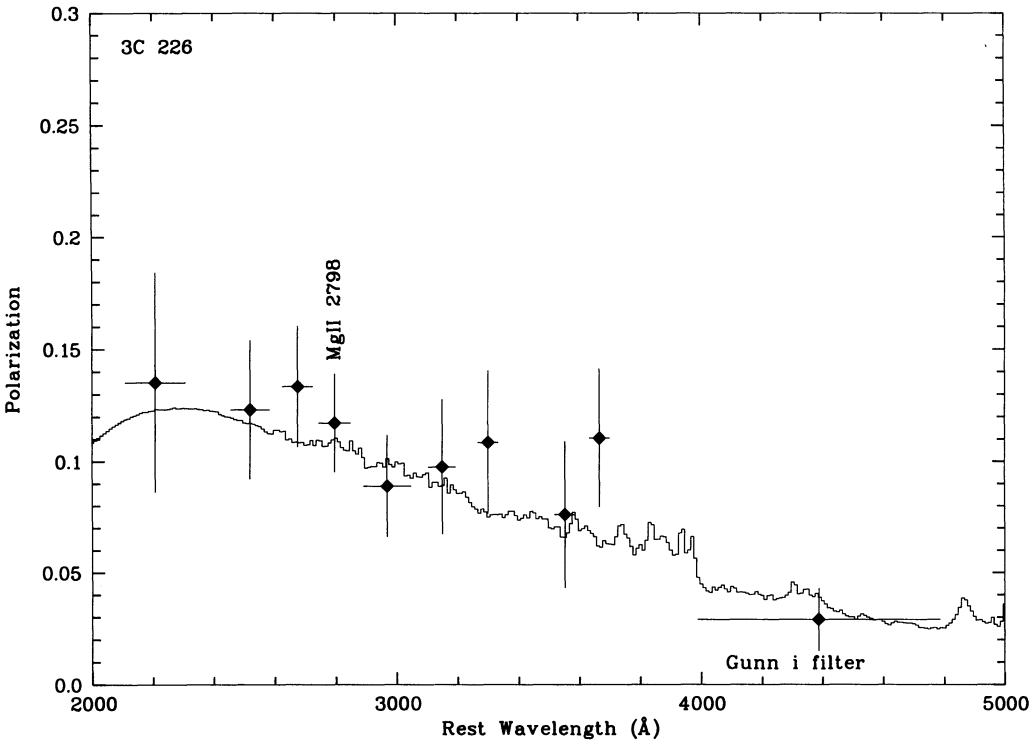


FIG. 2*a*

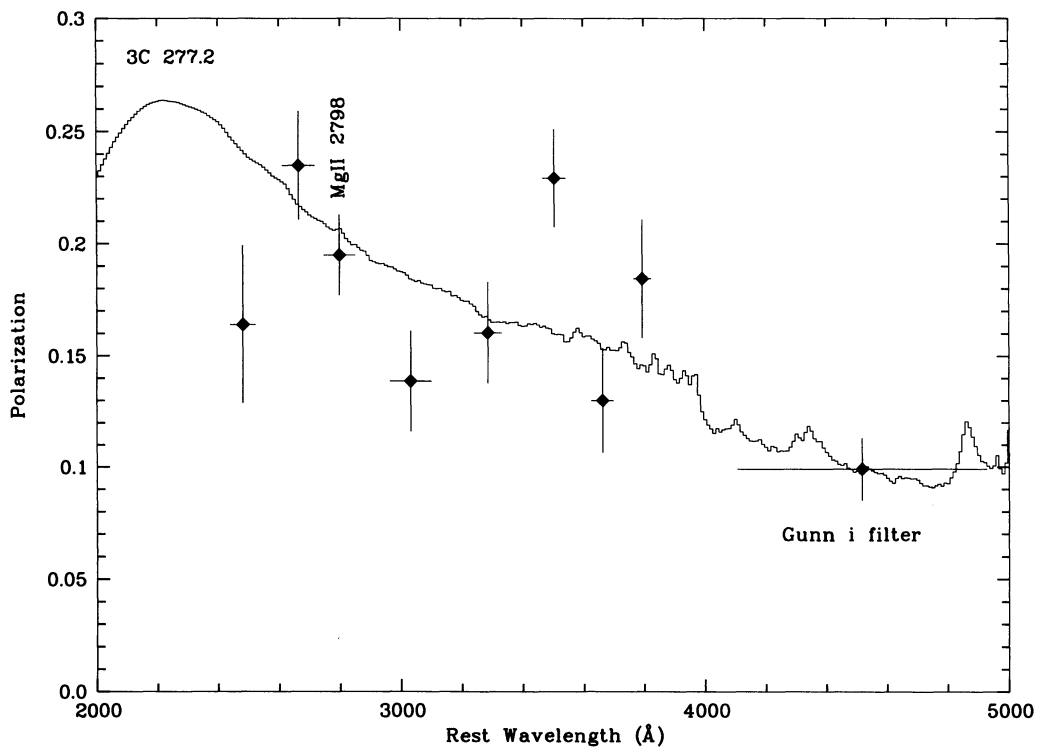


FIG. 2*b*

FIG. 2.—The degree of linear polarization for the continuum radiation as a function of rest frame wavelength. The dots with error bars show the data, while the continuous lines represent the polarization expected from our model (see § 4.6). The horizontal bars represent the measurement bands. The datum at 2800 Å contains also the Mg II line.

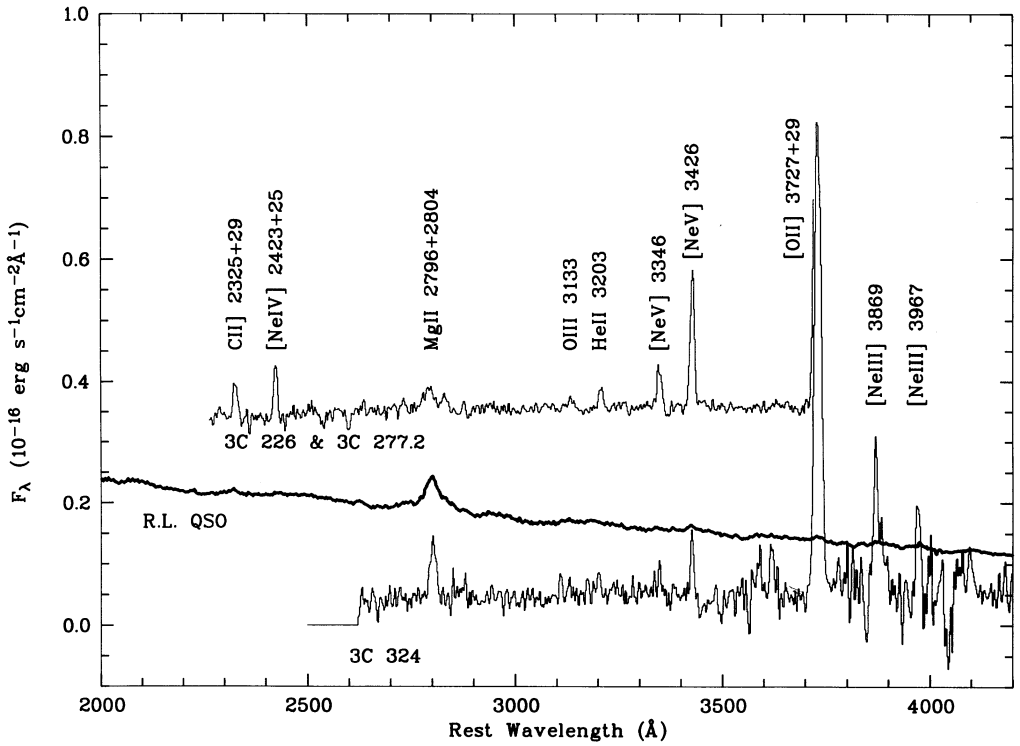


FIG. 3.—Total flux spectra for the three galaxies. The top spectrum show the average of the spectra of 3C 226 and 3C 277.2 and has been shifted up by $0.3 \times 10^{-16}$ ergs s$^{-1}$ cm$^{-2}$ Å$^{-1}$. The thick line is the typical spectrum of a radio-loud quasar from Cristiani & Vio (1990), shifted up by $0.06 \times 10^{-16}$ ergs s$^{-1}$ cm$^{-2}$ Å$^{-1}$.

tion at high redshift, although broad lines might have been seen in a few cases (C IV in B3 0744+464, McCarthy 1991; in MRC 0407−226, McCarthy et al. 1991; and in 53W 002, Windhorst et al. 1991). Figure 3 shows the total flux spectra of 3C 226 and 3C 277.2 averaged together, since they are almost identical, and of 3C 324. The line of Mg II λ2798 in 3C 226 and 3C 277.2 is clearly much broader than forbidden lines like [Ne V] λ3426, with a broadening of 3700 km s$^{-1}$ (FWHM). The width of the Mg II λ2798 line is similar to that measured in the averaged spectrum of radio-loud quasars (Cristiani & Vio 1990). The width of the Mg II λ2798 line in 3C 324 is only marginally larger than the forbidden lines in the spectrum integrated along the slit, but it does not show the marked tilt in velocity seen in the narrow-line gas (see Spinrad & Djorgovski 1984). We therefore conclude that the Mg II λ2798 line is broader than the forbidden lines in all three galaxies observed, consistent with the presence of a quasar-type spectrum. We also note that the equivalent width of the Mg II 2798 line in our galaxies (see Table 4) is equal, within the uncertainties, to that observed in radio-loud quasars (~30 Å in the rest frame; see Cristiani & Vio 1990).

This line is not only broad, but it is also polarized at about the same level as the nearby continuum (see Tables 3 and 4). In the case of 3C 324 the errors on the polarization are larger, given the higher sky level in the red. However, there is an indication the polarization of the Mg II line might be lower than that of the continuum.

### 3.4. *Narrow Forbidden Lines*

The spectra of the three galaxies, thanks to their signal-to-noise ratio, show a wealth of emission lines typical of radio galaxies. Their intensities and polarization [formally $S(\theta)$], after the subtraction of the continuum, are listed in Table 4. The polarization of those lines which are faint or affected by cosmic-ray hits could be given. The polarization of the narrow lines is consistent with zero and is inconsistent with the polarization of the continuum and of the broad lines. We note that even high-excitation lines such as [Ne V] 3426 are unpolarized and therefore presumably dominated by isotropic emission.

In the case of 3C we cannot confirm the presence of the lower redshift system at $z = 0.84$, suggested by Hammer, Nottale, & Le Fèvre (1986), since we do not see [O III] 5007 at that redshift in our spectrum extending further into the red. We also note that the lines ascribed to the $z = 0.84$ redshift system by Hammer et al. (1986) fall on strong sky features.

### 3.5. *Absorption Features*

The average spectrum of 3C 226 and 3C 277.2 (Fig. 4) shows a clear absorption feature at 2598 Å in the rest frame. This is present in all individual spectra of these two galaxies and has a rather large equivalent width (Table 4). Much less certain is the reality of the broader absorption feature around 2536 Å, which is present only in the spectra of 3C 277.2. Our spectrum of 3C 324 does not reach these short wavelengths.

## 4. DISCUSSION

### 4.1. *The Presence of a Hidden Quasar*

Our results strongly suggest the presence of an obscured quasar in the three distant radio galaxies which we have observed. By analogy with some nearby Seyfert 2 galaxies, type 1 AGN radiation is emitted anisotopically along the radio axis and scattered into our line of sight by some illuminated extranuclear medium. This beaming/scattering idea was proposed by Tadhunter, Fosbury, & di Serego Alighieri (1988) to explain the alignment effect in distant radio galaxies and has been

1994ApJ...431..123D

TABLE 4

SPECTROPOLARIMETRY OF EMISSION LINES

| LINE | 3C 226 | | | 3C 277.2 | | | 3C 324 | | |
|---|---|---|---|---|---|---|---|---|---|
| | $F_{obs}$ ($10^{-16}$ ergs s$^{-1}$ cm$^{-2}$) | $EW_{obs}$ (Å) | $S(\theta)$ | $F_{obs}$ ($10^{-16}$ ergs s$^{-1}$ cm$^{-2}$) | $EW_{obs}$ (Å) | $S(\theta)$ | $F_{obs}$ ($10^{-16}$ ergs s$^{-1}$ cm$^{-2}$) | $EW_{obs}$ (Å) | $S(\theta)$ |
| C II] 2325+29 ..... | 0.66 ± 0.1 | 19 ± 3 | ... | 1.9 ± 0.3 | 56 ± 8 | ... | ... | ... | ... |
| [Ne IV] 2423+25 ..... | 2.40 ± 0.1 | 107 ± 5 | −0.5% ± 5% | 1.8 ± 0.2 | 53 ± 6 | ... | ... | ... | ... |
| Mg II 2796+2803 ..... | 1.95 ± 0.2 | 62 ± 10 | 16 ± 4 | 2.7 ± 0.2 | 87 ± 9 | 20% ± 3% | 2.4 ± 0.1 | 81 ± 6 | 5% ± 8% |
| C II 2837+38 ..... | 0.64 ± 0.2 | 15 ± 5 | ... | 1.1 ± 0.2 | 25 ± 4 | ... | ... | ... | ... |
| O III 3133 ..... | ... | ... | ... | 0.7 ± 0.2 | 14 ± 4 | ... | ... | ... | ... |
| He II 3203 ..... | 0.72 ± 0.1 | 16 ± 3 | ... | 1.0 ± 0.2 | 18 ± 4 | ... | ... | ... | ... |
| [Ne V] 3346 ..... | 1.63 ± 0.1 | 33 ± 2 | −1 ± 5 | 1.7 ± 0.3 | 31 ± 6 | ... | ... | ... | ... |
| [Ne V] 3426 ..... | 4.50 ± 0.2 | 85 ± 4 | ... | 4.7 ± 0.1 | 83 ± 3 | 1 ± 2 | 1.3 ± 0.2 | 37 ± 6 | ... |
| [O II] 3727+29 ..... | ... | ... | ... | 11.6 ± 0.3 | 265 ± 8 | ... | 23.0 ± 0.5 | 600 ± 50 | 0 ± 2 |
| [Ne III] 3869 ..... | ... | ... | ... | ... | ... | ... | 6.4 ± 1.0 | 154 ± 20 | ... |
| [Ne III] 3968 ..... | ... | ... | ... | ... | ... | ... | 2.7 ± 0.5 | 82 ± 15 | ... |

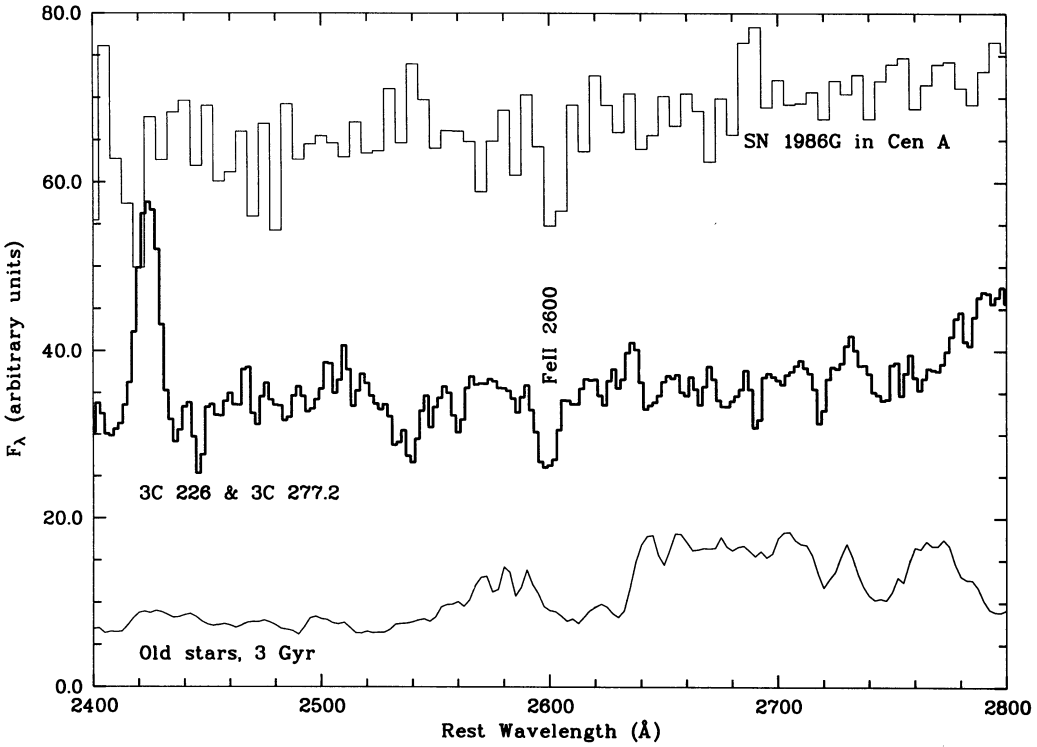


FIG. 4.—The absorption line at 2598 Å in 3C 226 and 3C 277.2. The average spectrum of the two galaxies has been shifted up by 20 units. Also shown is the *IUE* spectrum of the supernova SN 1986G in Cen A and a synthetic spectrum for a 3 Gyr old stellar population from Bruzual & Charlot (1993).

supported by subsequent imaging polarimetry (see Cimatti et al. 1993 and references therein). The principal evidence provided by the new results presented here is the presence of a polarized spectrum which has a continuum approximately flat in $f_\lambda$ (see Table 3) and a broad Mg II $\lambda$2798 line. Also the direction of the *E* vector is perpendicular to the radio/optical axis at all wavelengths observed in imaging polarimetry. We notice a difference with Seyfert 2 galaxies. In fact, in these objects the broad lines appear only in the *polarized* spectra (Antonucci & Miller 1985; Miller & Goodrich 1990), while in our radio galaxies the broad Mg II is already clear in the *total* spectra. This could be explained simply as a selection effect due to the different rest frame spectral range and dust scattering efficiency. In the UV the dilution by starlight becomes less important, and, if the scattering is due to dust, the scattering efficiency increases rapidly. In addition, the broad Mg II line in type 1 AGNs is usually not hidden below a narrow component, like the broad lines in the optical range (H$\beta$ and H$\alpha$). In this regard, it is interesting to notice that broad Fe II (2100, 2500, 2950 Å) emission lines were observed in the total spectrum of NGC 1068 with *IUE* (Snijders, Netzer, & Boksenberg 1986).

The presence of a scattered quasar spectrum with an Mg II equivalent width similar to that of direct quasar spectra shows that, even if a narrow blazar beam is present, the quasar dominates the scattered light because of its wider cone and higher total luminosity.

From our observations we can derive the column density of the scattering medium (dust or electrons) for each galaxies individually. In the case of dust scattering the dust column density $\eta$ can be obtained by

$$\eta = \frac{I_{\rm sca}}{I_{\rm QSO}} \frac{1}{\Omega \bar{S}}, \tag{2}$$

where $I_{\rm sca}/I_{\rm QSO}$ is the ratio of scattered to direct quasar light, $\Omega$ is the quasar cone solid angle (we assume a half-opening angle of 45°), $\bar{S}$ is the dust cross section per unit mass averaged over the cone (Cimatti et al. 1993). The ratio $I_{\rm sca}/I_{\rm QSO}$ is not known directly, but it can be expressed as the product of two observables:

$$\frac{I_{\rm sca}}{I_{\rm QSO}} = \frac{\kappa}{1+\kappa} \frac{I_{\rm RG}}{I_{\rm QSO}}, \tag{3}$$

where $\kappa = I_{\rm sca}/I_{\rm stars}$ is the ratio of scattered to stellar light in the observed *V* band (rest frame UV) derived from the spectral deconvolution (see § 4.6), and $I_{\rm RG}/I_{\rm QSO}$ is the flux ratio between quasar and radio galaxies at $z \sim 1$, as observed in the *V*-band Hubble diagram of the 3CR sample ($\Delta m \sim 4$; see Cimatti et al. 1993). With this method, we obtain $I_{\rm sca}/I_{\rm QSO} = 0.021$, 0.023, and 0.023, for 3C 226, 3C 277.2, and 3C 324, respectively. With the value of $\bar{S}$ from the scattering model discussed by Cimatti et al. (1983) we get $\eta = 3.4 \times 10^{-6}$ for 3C 226 and $3.7 \times 10^{-6}$ g cm$^{-2}$ for 3C 277.2 and 3C 324 for a mean scattering angle of 90°. Deriving the dust mass from $\eta$ requires some assumptions about the dust density distribution. Assuming a constant density within 10 kpc, decreasing as $1/r$ between 10 and 100 kpc and zero outside, we derive $M_{\rm dust} \sim 3 \times 10^8\ M_\odot$ for both galaxies. These masses are consistent both with the ones observed in nearby radio galaxies (Knapp & Patten 1991) and in high-redshift quasars (Andreani, La Franca, & Cristiani 1993).

In the case of electron scattering, the electron column number $n_e$ can be obtained from a formula equivalent to (2), where $\bar{S}$ is replaced by the Thomson scattering cross section for one electron. With the same assumptions as for the dust case, we get $n_e \sim 1.75 \times 10^{22}$ cm$^{-2}$, which corresponds to a column

density of ionized hydrogen of about $3 \times 10^{-2}$ cm$^{-2}$ for a total gas mass of $2.5 \times 10^{12}$ $M_\odot$. The very high gas mass required simply reflects the fact that dust has a much higher scattering efficiency per unit mass than electrons.

### 4.2. *The Scattering Medium*

In principle, the nature of the scattering medium can be diagnosed from the wavelength dependence of the polarization. In practice, however, there are relatively large errors in the measurements, and it is difficult to find ways of restricting the models which incorporate multiple scattering. In addition to the effects of grain composition and size distribution, the scattered spectrum from dusty clouds can vary greatly if any extinction is present. This can be seen by analogy with the variety of colors of the twilight sky which are produced by Rayleigh scattering with varying pathlengths through an illuminated and a shadowed scattering medium. Our observations do, however, exclude a strong wavelength dependence of polarization in the rest frame UV.

Scattering by electrons in a hot intracluster halo would broaden the incident spectrum by about 30,000 km s$^{-1}$ (Fabian 1989), effectively smearing out completely any spectral features.[4] The fact that broad polarized lines are observed with similar widths to those observed in quasar spectra proves that scattering by hot electrons is not the dominant process. In the previous section, we have shown that scattering by cold electrons over large distances would require unreasonably large gas masses. However, if the electron density is high in the nuclear regions, the quantity of gas necessary can be greatly reduced. For example, if the electron density is constant within 100 pc and zero outside, the required gas mass would be only $5.6 \times 10^6$ $M_\odot$. Therefore, one scattering by hot electrons in a massive halo is excluded, electron scattering can only dominate over dust scattering in the very central regions—as in the case of NGC 1068 (Miller & Goodrich 1990; Code et al. 1993)—and cannot explain the extranuclear polarization which has been directly observed in a few distant radio galaxies (3C 368, 3C 265, and 1336+020).

An additional argument in favor of dust scattering concerns the observed degree of polarization in radio galaxies. Assuming a range of scattering angles between 45° and 90° (Barthel 1989), Thomson scattering would produce a degree of polarization significantly higher than observed—in the range of about 20% to 50% (Miller & Goodrich 1990)—while Galactic dust grains produce a polarization of between 10% and 20% (Cimatti et al. 1993, 1994), consistent with observations. Therefore, Thomson scattering is a poor model in the case of 3C 226, while it cannot be excluded in 3C 277.2 nor in 3C 324 simply on the basis of the degree of polarization. Electron scattering would require the presence of an unpolarized UV source to dilute the intrinsic polarization. We will show in § 4.4 that there is no strong evidence for such dilution.

### 4.3. *Geometrical Constraints on the BLR and NLR*

Within the uncertainties of these difficult observations, our results on the polarization imply that the continuum and broad lines are emitted anisotropically from the quasar, while the narrow emission lines are essentially isotropic. The anisotropy of the broad lines must be predominantly due to nuclear obscuration while, for the continuum, the addition of an intrinsic beaming is possible—the blazar component. The most basic model, with a nonstellar continuum source and a broad-line region (BLR) capable of falling entirely within the obscuring structure and an narrow-line region (NLR) which is entirely outside it, is already showing signs of being oversimplified. There is evidence for an extended source of AGN continuum, some fraction of which can be seen directly even when the BLR is totally obscured (see Binette, Fosbury, & Parker 1993; Tran, Miller, & Kay 1992; Cimatti et al. 1994; Antonucci 1993). This can result in the BLR polarization being larger than that of the continuum, even without dilution by starlight. Also, the failure of the Jackson-Browne test for [O III] (Jackson & Browne 1990) and its success for [O II] (Hes, Barthel, & Fosbury 1993) suggests that part of the so-called NLR, at least those lines from a higher ions and with a large critical density for collisional de-excitation, can come from so close to the classical BLR that they also can suffer obscuration anisotropy. Nevertheless, our observations also show that the high-ionization lines, such as [Ne V], are unpolarized and therefore isotropic.

### 4.4. *The Diluting Radiation*

The sudden drop in the degree of polarization observed both in 3C 226 and 3C 277.2 longward of 4000 Å points to the presence of diluting radiation with a strong 4000 Å break. The same effect has been noticed statistically by examining the polarization measurements of all radio galaxies with $z \geq 0.1$ (Cimatti et al. 1993) but is seen here much more clearly in the spectropolarimetric data of individual galaxies. We interpret this drop as dilution by the light of the host galaxy which contains an evolved stellar population. From the polarization drop, we can estimate that the 4000 Å break in the diluting radiation should be $B_\nu = 5.5 \pm 3.9$ for 3C 226 and $B_\nu = 3.3 \pm 1.0$ for 3C 277.2 (see Bruzual 1983 for the definition). The errors in these estimates are large, and the value we derive is not completely model independent since it depends on the relative amount of diluting flux. This is, however, a strong indication of the presence of an evolved stellar population.

This result conflicts with that of Hammer, Le Févre, & Angonin (1993), who do not see the break in the average spectrum of 10 distant radio galaxies, including 3C 226. They argue that $B_\nu$ must be less than 1.1 on average for the galaxies they have observed. We have already discussed that the data presented by Hammer et al. (1993) are not in conflict with the presence of a diluted old stellar population (Cimatti et al. 1994). We only add that our method based on polarization measures the break on the nonscattered component of the light, while Hammer et al. (1993) measure it on the total radiation, not taking into account that an eventual strong break from an evolved stellar population will be diluted by the scattered light. In principle, the value of $B_\nu$ allows the estimate of the age of the stellar population (Bruzual & Charlot 1993), but the large errors in the case of 3C 226 prevent a meaningful age determination in this way. For 3C 277.2, a value of $B_\nu \geq 2$ indicates a stellar age which must be larger than 2 Gyr.

The total fluxes which we measure on either side of the 4000 Å break (Fig. 5) are consistent with the presence of the old stellar population derived from the spectral model in § 4.6 but are of little use to directly constrain the value of the break in the diluting radiation.

The fact that the Mg II $\lambda$2798 line is polarized at a level not higher than that of the nearby continuum limits the amount of diluting UV radiation, since it is directly consistent with

[4] Actually the Doppler-broadening produced by electrons at the temperature $T$, scattering at an angle $\theta$, is $\sigma = 41600\sqrt{(1 - \cos\theta)[T/(7 \times 10^7\ \mathrm{K})]}$ km s$^{-1}$.

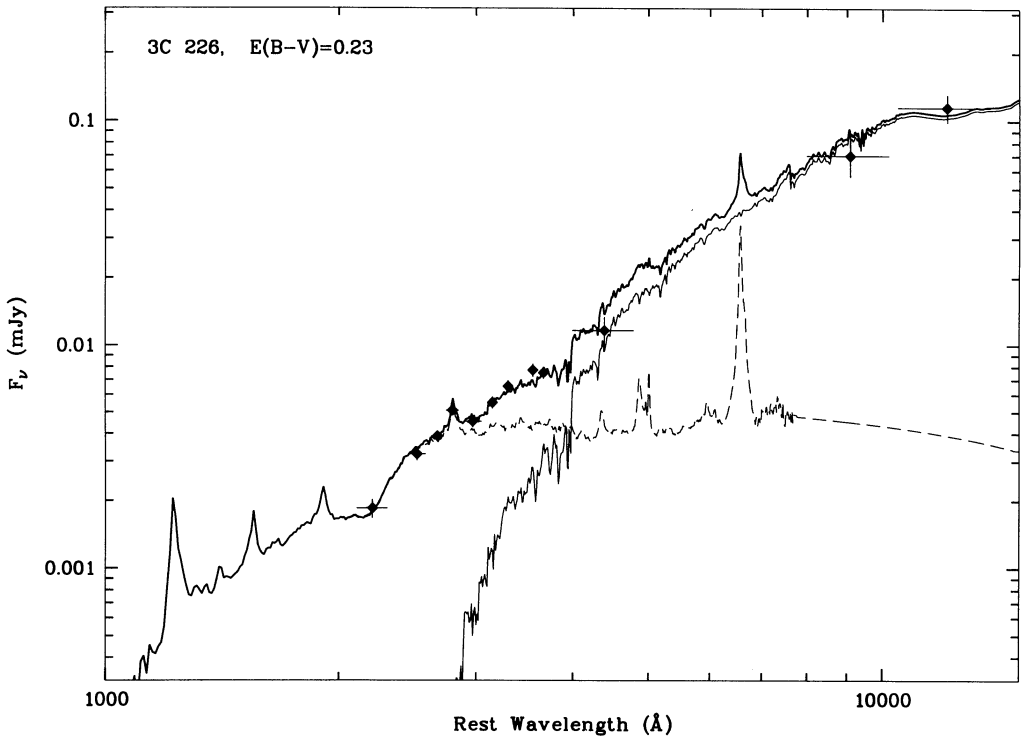


FIG. 5*a*

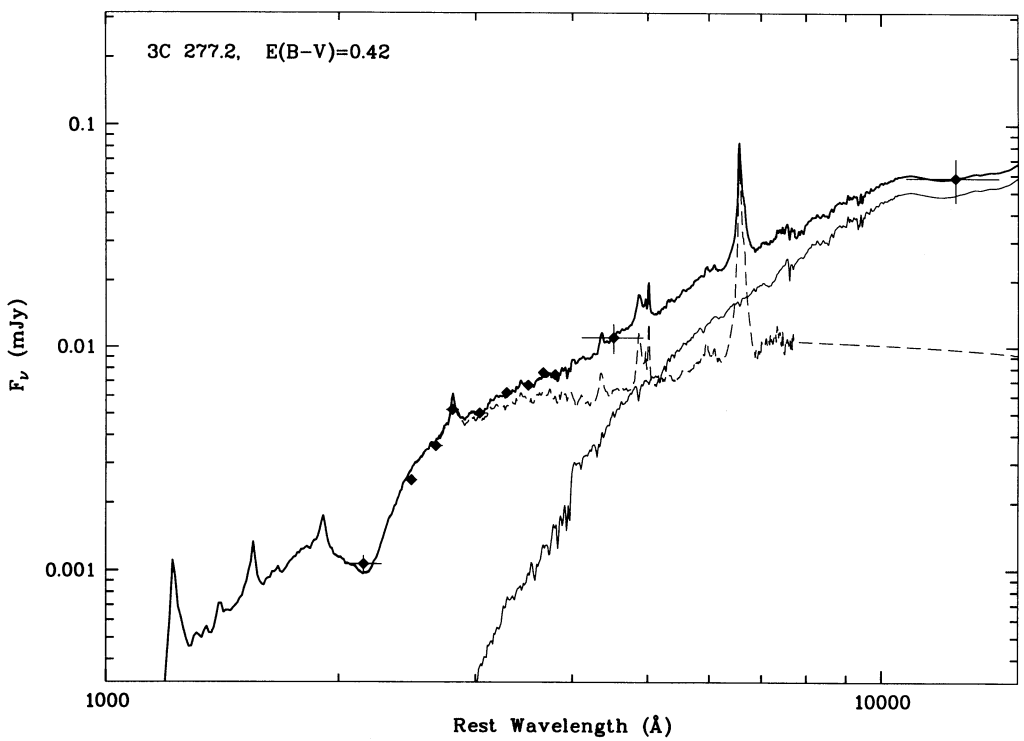


FIG. 5*b*

FIG. 5.—The best fitting two-component models of the spectral energy distribution. The dots with error bars are the data, and the horizontal bars represent the measurement bands. The lines represent the best fitting spectral models: the thin line is the spectrum of the stellar population (age of 4, 2, and 5 Gyr for 3C 226, 3C 277.2, and 3C 324, respectively), the dashed line is the spectrum of the dust-scattered quasar, and the thick line is the sum of these two components.

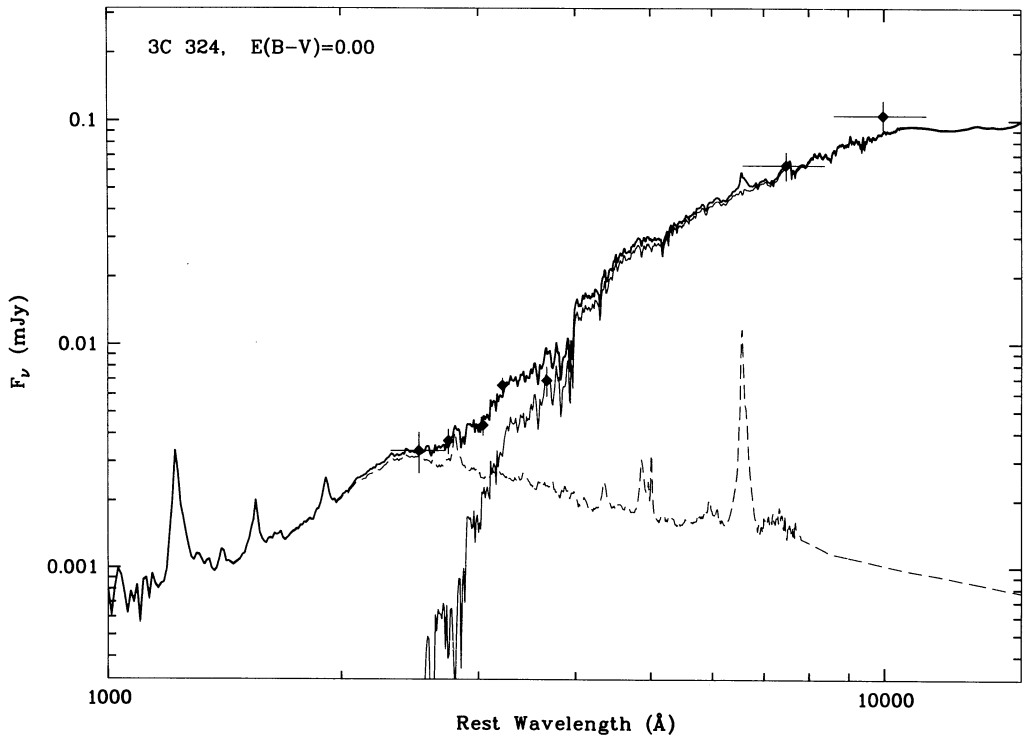


FIG. 5c

scattering of a type 1 spectrum. Any emission-line–free diluting radiation would cause the degree of polarization to become higher at the Mg II λ2798 line where the scattered spectrum is stronger. With data of the present precision, the solution for the ratio between the diluting and the scattered radiation from the line and continuum polarization measurements is a rather ill-constrained mathematical problem, and it is only in the case of 3C 277.2, which has the largest polarization, that we can derive a meaningful result for this ratio of $0.15 \pm 0.5$. Although this kind of approach can, in principle, limit the quantity of unpolarized ultraviolet light from young stars, its usefulness is limited by the attainable accuracy of the measurements and also by the possible presence of unobscured nonstellar AGN continuum (see § 4.3 above).

Another independent indication that the dilution around 2800 Å is small comes from the fact that the equivalent widths of the Mg II 2798 are equal, within the uncertainties, to that observed in radio-loud quasars.

### 4.5. *The Absorption Feature*

F and G type stars have a Fe II λ2600 absorption (Fanelli et al. 1990). Nevertheless these stars emit very little in the UV, and the UV dilution is probably small (see § 4.4). Therefore, we exclude that the high equivalent width absorption line that we observe is of stellar origin. We interpret it as due to interstellar Fe II λ2600.18, which is the second strongest UV interstellar absorption line after Mg II λ2796+2804, which is filled by emission in our galaxies (Kinney et al. 1993). Other Fe II absorption lines might be present in our spectrum, like a blend of 2374.4 and 2382.8, while the line at 2586.7 could be blended with the 2600.2, and the line at 2344.2 might be hidden under the C II] emissions. The rest frame equivalent width of the 2600 Å line in our spectra is $8 \pm 2$ Å, larger than normally observed (Kinney et al. 1993). However, such a line is seen with comparable strength in the *IUE* spectrum of the supernova SN 1986G in the dust lane of Cen A (Fig. 4). The unusual strength of this interstellar Fe II line in our radio galaxies could be due to the fact that iron is less depleted than normal because the dust grains are destroyed, e.g., by the intense nuclear UV radiation. It is conceivable that the quasar light first travels through an interstellar medium poor of dust grains, but rich of iron, and then is scattered by dust at larger distances from the nucleus, where the UV flux is reduced below dust survival levels. Also, several components at different velocities, which we see blended in our low-resolution spectra, could increase the equivalent width above galactic levels.

### 4.6. *A Spectral Model*

The spectral energy distribution of the continuum radiation of 3C 226, 3C 277.2, and 3C 324 is defined by our optical spectrophotometry, by our Gunn *i* flux, and by infrared photometric data from Lilly & Longair (1984) and Rigler et al. (1992). In particular, we use the infrared photometry with the aperture which more closely matches the optical data. In the case of 3C 324 we extend the data in the UV with the line-free *V* magnitude of Spinrad & Djorgovski (1984). The Gunn *i* flux was obtained by integrating the galaxy image with an aperture $9'' \times 2''$ equal in orientation and area to that of the slit used in spectropolarimetry. The Gunn *i* flux has been corrected for the contamination by emission lines (Hβ, Hγ, Hδ, and He II λ and [O III] 4959+5007) present in the band by using the typical narrow-line ratios of radio galaxies (McCarthy 1993). The lines contribute to the observed flux by 19.7% and 33.7% in 3C 226 and 3C 277.2, respectively. Also, the near-infrared bands (*H* and *K*) contain some emission lines. However, given the very broad bandwidths of these filters and the relative weakness of the lines, the contamination is small. According to typical infrared line ratios observed in AGNs (Osterbrock, Shaw, &

Veilleux 1990; Oliva et al. 1994), we estimate a 2% contribution to the H flux by [S III] 9069+9531 in 3C 226, $\leq$0.5% to the $K$ flux by Pa$\beta$ both in 3C 226 and 3C 277.2, and $<$0.5% to the $H$-band flux by [Ar III] 7136 and 1.4% to the $K$ flux by [S III] 9069+9531 and He I 10830 in 3C 324.

The resulting spectral energy distributions were modeled by using a two-component model consisting of a dust-scattered quasar and single stellar population. We have used the typical spectrum of a radio-loud quasar given by Cristiani & Vio (1990) scattered by dust with a galactic compósition and grain-size distribution, adopting Mie single scattering (Cimatti et al. 1993). For the stellar component we use the synthetic spectra of simple stellar populations (instantaneous burst) of Bruzual & Charlot (1993) and Salpeter IMF over a range of 0.1–125 $M_\odot$. We have also introduced a certain amount of dust extinction, to decrease the UV light. Nevertheless, at least part of this extinction is probably due to the fact that the scattering cross section that we have used has a strong 2200 Å feature, while recent data show that this feature is only present in absorption, but not in scattering (e.g., Witt et al. 1992).

The introduction of some extinction is realistic according to the observations of neutral hydrogen and cold ISM nearby radio galaxies (van Gorkom et al. 1989; Mirabel 1989; Golombek, Miley, & Neugebauer 1988; Knapp, Bies, & van Gorkom 1990; Knapp & Patten 1991). The hydrogen column density $N_H$ can reach $10^{21}$ cm$^{-2}$, implying, if the ISM is Galactic, $E_{B-V}$ up to $\sim$0.2 mag. If the interstellar medium (ISM) of high-$z$ radio galaxies has similar properties, the extinctions required by our dust scattering model and spectral fitting are reasonable, especially if it is reduced in the case that the 2200 Å feature is due only to absorption. To this regard it is also important to notice that cold dust is required to explain the millimeter observations of high-redshift quasars (Andreani et al. 1993), and that direct evidence of dust is provided by the small Ly$\alpha$/N V $\lambda$1140 flux ratio in a radio galaxy at $z = 2.3$ (Miley 1994). Finally, we mention that a 2200 Å dip, probably due to dust extinction, is observed in a high signal-to-noise ratio composite quasar spectrum (Francis et al. 1991).

The results of our spectral models are shown in Figure 5, which gives also the adopted amount of extinction and the age of the stellar population. Clearly the model fits the data of all three galaxies very well (best $\chi^2_{red} = 0.73$, for age 5 Gyr, for 3C 226; $\chi^2_{red} = 1.45$, for age 2 Gyr, for 3C 277.2; and $\chi^2_{red} = 1.43$, for 5 Gyr, for 3C 324). The age of the stellar population that gives an acceptable fit at the 5% level of significance is constrained to be larger than 3 Gyr for 3C 226, between 0.5 and 2.5 Gyr for 3C 277.2, and larger than 2 Gyr for 3C 324. The presence of an evolved stellar population is also consistent with the drop of the polarization beyond 4000 Å. The polarization predicted by our model for the total light is shown in Figure 2 and is consistent with the observed values.

We have obtained the $K$-corrected absolute magnitudes $M_V$ of the host galaxies from the pure stellar components derived by the spectral deconvolution and compared them to those of nearby galaxies. We have used $H_0 = 100$ and $q_0 = 0$ in order to be consistent with the comparison sample. The magnitudes not corrected for the internal reddening are $-22.3$, $-21.1$, and $-23.9$, respectively, for 3C 226, 3C 277.2, and 3C 324, and they become $-23.0$ and $-22.4$ for the first two galaxies, if the stellar SEDs are corrected for the extinction derived from the fit to the scattered light, although we have doubts on its physical soundness and on its applicability into the stellar component. These luminosities are consistent with those of nearby powerful radio galaxies and luminous ellipticals, 3C 324 being at the bright end of the range (Smith & Heckman 1989; Smith, Heckman, & Illingworth 1990).

The apparent $V$ magnitude that the hidden quasars would have if viewed directly is easily obtained from the observed magnitude of the galaxy and the ratio of scattered to direct quasar light derived in § 4.1, since our spectral model shows that in rest frame range redshifted to the $V$ band the light of the galaxy is dominated by the scattered quasar. We obtain $V = 17.5$, 17.4, and 18.5 for the quasar in 3C 226, 3C 277.2, and 3C 324, respectively, well within the range of observed magnitudes for (3C) quasars at the same redshift.

### 4.7. *The Constancy of the Polarization*

The consistency of the spectropolarimetry performed in 1993 March with the previous imaging polarimetry in the same wavelength range performed in the period 1989–1992 (see Tables 1 and 3) limits the amount of polarization variability over a timescale of the order of 1 yr. While this is not, itself, a strong constraint on the origin of the polarization, it is consistent with the idea that the contribution of intrinsic variable polarization in the incident quasar spectrum—the blazar component—is insignificant in direct light.

### 4.8. *Implications for the Alignment Effect*

The idea that the alignment effect in distant radio galaxies, discovered by McCarthy et al. (1987) and Chambers, Miley, & van Breugel (1987), could be due to scattered nuclear light was stimulated by the discovery of an extremely blue and highly polarized off-nuclear continuum in the low-redshift radio galaxy PKS 2152−69, which appears to be reflected nuclear radiation (di Serego Alighieri et al. 1988), and was first suggested by Tadhunter et al. (1989), who predicted that distant radio galaxies would be polarized. This prediction was soon confirmed by the observations of di Serego Alighieri et al. (1989) and others following, giving strong support to the scattering explanation for the alignment effect.

The data presented in this paper reinforce this explanation by removing, at least for the observed galaxies, one difficulty put forward by the supporters of the alternative jet-induced star-formation hypothesis, that is, the supposed absence of polarized broad emission lines (e.g., Miley 1994). In our view, if distant radio galaxies harbor a hidden source of ionizing radiation, as is generally accepted to explain the aligned line emission, it would be difficult to avoid scattering and therefore also aligned and polarized UV continuum.

Our model does not necessarily exclude that some fraction of the aligned UV excess might be produced by young stars, since their spectral energy distribution is not too different from that of a scattered quasar (Cimatti et al. 1994). However, we have remarked in § 4.4 that the similarity of the degree of polarization for the Mg II 2798 line and for the nearby continuum and of the observed Mg II 2798 equivalent width with that of quasars points to a small dilution in the UV and therefore limits the radiation from young stars, e.g., to less than about one-third of the total radiation around 2800 Å in the case of 3C 277.2.

About the two main competing, but not mutually exclusive, explanations for the alignment effect—i.e., scattering of anisotropic nuclear radiation and jet-induced star formation—we note that the perpendicular polarization clearly observed in a dozen of distant radio galaxies demonstrates the presence of

scattered radiation, while the direct evidence for young stars is only marginal so far (Chambers & McCarthy 1990).

## 5. SUMMARY AND OUTLOOK

We have presented the results of spectropolarimetry of three distant radio galaxies with redshift around one, complemented by imaging polarimetry, which are summarized as follows.

1. The broad polarized Mg II 2798 emission lines with a width consistent with that observed in quasars, together with the flat perpendicularly polarized continuum demonstrate the presence of a hidden quasar, whose type 1 spectrum is visible by scattering, probably by dust.
2. The fact that the broad Mg II 2798 has the width observed in quasars excludes that scattering is due to electrons from a hot halo, since these would smear out the line.
3. The narrow forbidden emission lines are not polarized, and are therefore emitted mostly isotopically.
4. The sudden drop in the degree of polarization to the red of 4000 Å points to the presence of diluting radiation with a strong 4000 Å break, consistent with an evolved stellar population.
5. The strong absorption feature at 2598 Å, probably due to interstellar Fe II, suggests the presence of an interstellar gas with unusual abundances and large velocities.
6. A model consisting of a dust-scattered quasar and of a Gyr-old stellar population reproduces well the spectral energy distribution and the polarization for all three observed galaxies.
7. The amount of dust, the luminosity of the quasar, and the luminosity of the stellar component are all consistent with those expected in the framework of the unified model of AGN.
8. Our results add strength to the scattering explanation for the alignment effect.

Our simple two-component model suggests that the light from distant radio galaxies is dominated by the scattered quasar only up to about 4000–5000 Å in the rest frame and that most of the radiation observed beyond 1 $\mu$m for objects at $z \sim 1$ or beyond 1.5 $\mu$m for $z \sim 2$ should be stellar. In this simple scheme, no polarization nor alignment are expected in the $K$-band. Some infrared alignment has nevertheless been observed, but the amount of aligned light is smaller than in the optical (Rigler et al. 1992), has a different morphology, pointing to a different origin, and shows an even more precise alignment with the radio axis (Dunlop & Peacock 1993). Also, some infrared polarization has been detected in two of the four distant radio galaxies observed (Elston & Jannuzi 1994), although at a smaller level and different position angle than in the optical, again pointing to a different origin. It is clearly beyond the scope of this paper to explain the infrared morphology and polarization of distant radio galaxies, and we have traded the simplicity of our model for the complications necessary to fit every aspect at every wavelength. We can only comment that electron scattering near the nucleus might play a role in the infrared and/or the reduced extinction at longer wavelength might allow to see the nuclear regions directly through aligned dust grains. More infrared polarimetry, particularly if it were spatially resolved, would be very useful to clarify this issue.

With the advent of 8–10 m class telescopes, work similar to the one presented in this paper can be extended to a larger sample of distant radio galaxies and refined to provide a more precise definition of the incident quasar spectrum, of the scattering parameters, and of the age of the stellar population.

We thank Buell Jannuzi, Simon Lilly, Tino Oliva, Marco Salvati, Sandra Savaglio, Roberto Viotti, and Adolf Witt for useful discussions, Stefano Cristiani for providing the typical spectrum of quasars, and Robert W. Goodrich, the referee, for helpful comments.

## REFERENCES

Andreani, P., La Franca, F., & Cristiani, S. 1993, MNRAS, 261, L35
Antonucci, R. 1993, ARA&A, 31, 473
Antonucci, R. R. J. 1984, ApJ, 278, 499
Antonucci, R. R. J., & Miller, J. S. 1985, ApJ, 297, 621
Baldwin, J. A., & Stone, R. P. S. 1984, MNRAS, 206, 241
Barthel, P. D. 1989, ApJ, 336, 606
Binette, L., Fosbury, R. A. E., & Parker, D. 1993, PASP, 105, 1150
Bruzual, A. G. 1983, ApJ, 273, 105
Bruzual, A. G., & Charlot, S. 1993, ApJ, 405, 538
Chambers, K. C., & McCarthy, P. J. 1990, ApJ, 354, L9
Chambers, K. C., & Miley, G. K. 1990, in Evolution of the Universe of Galaxies, ed. R. G. Kron (ASP Conf. Ser., 10), 373
Chambers, K. C., Miley, G. K., & van Breugel, W. 1987, Nature, 329, 604
Cimatti, A., di Serego Alighieri, S., Field, G. M., & Fosbury, R. A. E. 1994, ApJ, 422, 562
Cimatti, A., di Serego Alighieri, S., Fosbury, R. A. E., Salvati, M., & Taylor, D. 1993, MNRAS, 264, 421
Clarke, D., & Stewart, B. G. 1986, Vistas Astron., 29, 27
Code, A. D., et al. 1993, ApJ, 403, L63
Cristiani, S., & Vio, R. 1990, A&A, 227, 385
di Serego Alighieri, S., Binette, L., Courvoisier, T. J.-L., Fosbury, R. A. E., & Tadhunter, C. N. 1988, Nature, 334, 591
di Serego Alighieri, S. 1989, in ESO Conf. and Workshop Proc. No. 31, 1st ESO/ST-ECF Data Analysis Workshop, ed. P. P. Grosbøl P. (Garching bei München: ESO), 157
di Serego Alighieri, S., Cimatti, A., & Fosbury, R. A. E. 1993, ApJ, 404, 584
di Serego Alighieri, S., Fosbury, R. A. E., Quinn, P. J., & Tadhunter, C. N. 1989, Nature, 341, 307
Dunlop, J. S., & Peacock, J. A. 1993, MNRAS, 263, 936
Elston, R., & Jannuzi, B. T. 1994, in preparation
Fanelli, M. N., O'Connell, R. W., Burstein, D., & Wu, C.-C. 1990, ApJ, 364, 272
Fabian, A. C. 1989, MNRAS, 238, 41P
Fosbury, R. A. E., Cimatti, A., & di Serego Alighieri, S. 1993, Messenger, 74, 11
———. 1994, in preparation
Francis, P. J., Hewett, P. C., Foltz, C. B., Chaffee, F. H., Weymann, R. J., & Morris, S. L. 1991, ApJ, 373, 465
Golombek, D., Miley, G. K., & Neugebauer, G. 1988, AJ, 95, 26
Hammer, F., Le Fèvre, O., & Angonin, M. C. 1993, Nature, 362, 324
Hammer, F., Nottale, L., & Le Fèvre, O. 1986, A&A, 169, L1
Hes, R., Barthel, P. H., & Fosbury, R. A. E. 1993, Nature, 326, 362
Jackson, N., & Browne, I. W. A. 1990, Nature, 343, 43
Kinney, A. L., Bohlin, R. C., Calzetti, D., Panagia, N., & Wise, R. F. G. 1993, ApJS, 86, 5
Knapp, G. R., Bies, W. E., & van Gorkom, J. H. 1990, AJ, 99, 476
Knapp, G. R., & Patten, B. M. 1991, AJ, 101, 1609
Lilly, S. J., & Longair, M. S. 1984, MNRAS, 211, 833
McCarthy, P. J. 1991, AJ, 102, 518
———. 1993, ARA&A, 31, 693
McCarthy, P. J., van Breugel, W., Kapahi, V. K., & Subrahmanya, C. R. 1991, AJ, 102, 522
McCarthy, P. J., van Breugel, W., Spinrad, H., & Djorgowski, S. 1987, ApJ, 321, L29
Meisenheimer, K., & Hippelein, H. 1992, A&A, 264, 455
Melnick, J., Dekker, H., & D'Odorico, S. 1989, ESO Operating Manual No. 4, EFOSC (ESO Faint Object Spectrograph and Camera), (Garching bei München: ESO)
Miley, G. 1994, in The Physics of Active Galaxies, ed. G. V. Bicknell, M. A. Dopita, & P. J. Quinn (San Francisco: ASP), in press
Miller, J. S., & Goodrich, R. W. 1990, ApJ, 355, 456
Miller, J. S., Goodrich, R. W., & Mathews, W. 1991, ApJ, 378, 47
Mirabel, F. 1989, ApJ, 340, L13
Oliva, E., Salvati, M., Moorwood, A. F. M., & Marconi, A. 1994, A&A, submitted
Osterbrock, D. E., Shaw, R. A., & Veilleux, S. 1990, ApJ, 352, 561

Padovani, P., & Urry, C. M. 1992, ApJ, 387, 449
Rigler, M. A., Lilly, S. J., Stockton, A., Hammer, F., & Le Fèvre, O. 1992, ApJ, 385, 61
Serkowski, K., Mathewson, D. S., & Ford, V. L. 1975, ApJ, 196, 261
Smith, E. P., & Heckman, T. M. 1989, ApJ, 341, 658
Smith, E. P., Heckman, T. M., & Illingworth, G. D. 1990, ApJ, 356, 299
Snijders, M. A. J., Netzer, H., & Boksenberg, A. 1986, MNRAS, 222, 549
Spinrad, H., & Djorgovski, S. 1984, ApJ, 280, L9
Stone, R. P. S. 1977, ApJ, 218, 767
Stone, R. P. S., & Baldwin, J. A. 1983, MNRAS, 204, 347
Tadhunter, C. N., Fosbury, R. A. E., & di Serego Alighieri, S. 1988, in Proc. the Como Conference, BL Lac Objects, ed. L. Maraschi, T. Maccacaro, & M. H. Ulrich (Berlin: Springer-Verlag), 79
Tadhunter, C. N., Scarrott, S. M., Draper, P., & Rolph, C. 1992, MNRAS, 256, 53P
Tran, H. D., Miller, J. S., & Kay, L. E. 1992, ApJ, 397, 452
van Gorkom, J. H., Knapp, G. R., Ekers, R. D., Ekers, D. D., Laing, R. A., & Polk, K. S. 1989, AJ, 97, 708
Visvanathan, N. 1966, Ph.D. thesis, Australian National Univ.
Wardle, J. F. C., & Kronberg, P. P. 1974, ApJ, 194, 249
Windhorst, R. A., et al. 1991, ApJ, 380, 362
Witt, A. N., Petersohn, J. K., Bohlin, R. C., O'Connell, R. W., Roberts, M. S., Smith, A. M., & Stecher, T. P. 1992, ApJ, 395, L5